

## Valence states, impurities and electrocrystallization behaviors during molten salt electrorefining for preparation of high-purity titanium powder from sponge titanium

Qi-gang WENG, Rui-di LI, Tie-chui YUAN, Jian LI, Yue-hui HE

State Key Laboratory of Powder Metallurgy, Central South University, Changsha 410083, China

Received 28 October 2013; accepted 20 January 2014

**Abstract:** High-purity titanium powder was prepared by molten salt electrorefining from sponge titanium in NaCl–KCl–TiCl<sub>x</sub> salts. The titanium valence, purity and electrocrystallization during electrolysis process were studied. The XPS analysis showed that the titanium valences are mainly +4, +3 and +2 at the earlier, medium and later stages of electrolysis, respectively. During the electrolysis process, the contents of impurities Si, Cr, Mn, Al vary little, and the contents of impurities Fe, Cu, Ni decrease markedly, while the contents of impurities O, N, H increase obviously. The residual impurities are usually distributed in small tunnel of dendritic crystals. Enhancing the electrolysis temperature and prolonging the electrolysis time can increase the titanium particle size. The TEM analysis showed that the electrodeposited titanium is not a single crystal, but contains many nanostructured grains and subgrains, with grain size of 100–500 nm. The electrolysis mechanisms were also discussed.

**Key words:** molten salt electrolysis; high-purity titanium; powder; valence; electrocrystallization

### 1 Introduction

High-purity titanium powder is the titanium material with purity reaching or exceeding 4N grade (99.99%). In addition to the universal properties of titanium, such as high melting point, low density, good corrosion resistance, and nonmagnetic, the high-purity Ti powder possesses excellent mechanical, electronic, biological, adsorbent properties, etc [1,2]. Therefore, the high purity Ti powder is now widely used in powder metallurgy, biofabrication, integrated circuit target, high vacuum suction, etc. Up to now, the demand for high purity Ti powder is rapidly increasing with the development of various high-tech areas. Consequently, investigation into the preparation of high-purity Ti powder has profound importance [3].

At present, the traditional procedures for preparation of high-purity titanium powder have two main steps. The first step is the preparation of high purity bulk Ti material from raw Ti by hot reduction (Kroll method) [4–6], thermal cracking of Ti halogenated salt [7], electron beam fusion [8], molten salt electrolysis of

TiCl<sub>4</sub> [2,9,10], electrochemical reduction of TiO<sub>2</sub> [11–15]. The second step is atomizing the high purity Ti melt. However, the conventional procedures have the following insufficiencies. First, the traditional procedures are complex trival, low yield rate, limiting the practical industry production. Second, the traditional methods have high requirements for raw material, which inevitably increase the cost. Third, the two steps would easily lead to the impurities pollution, which seriously deteriorate the purity of Ti powder. Fourth, the traditional methods have a purification limitation that some impurities could not be removed thoroughly. For example, the electron beam fusion could not easily remove the Fe, Ni, O elements. Fifth, the powder characterisations by traditional methods could not be controlled easily. Above all, it is obvious that the traditional Ti preparation produces are currently severely hindering the development of Ti industry, and a new preparation method for preparation high-purity Ti is necessary.

The molten salt electrolysis (MSE), not only can produce high purity Ti from Ti sponge, but also can prepare Ti powder flexibly by cathodic reduction of the Ti from ion to crystal, exhibiting advantages in the

preparation of high-purity Ti powder. Our previous work has preliminary reported preparing high-purity titanium by MSE [10]. However, the valence variation, electrocrystallization mechanisms, and the electrocrystallization are not investigated, although the above scientific issues are very important in deeply understanding and controlling the electrolytic powder quality. In this work, the high-purity Ti powder is prepared by MSE. The valence state evolution of Ti ion, impurities distribution and the effects of electrolytic conditions on the powder characterizations are studied.

## 2 Experimental

Figure 1 shows the molten salt electrolysis apparatus schematically. The MSE equipment included charging, electrolytic and vacuum systems. The anode was a nickel basket which contained titanium sponge and the cathode was the pure titanium. During the electrolysis process, at the anode, the Ti sponge lost electron and became low valence Ti ion, accordingly deposited on the cathode by reduction reaction, and thus Ti powder can be obtained. The following is the detailed experimental procedures. First, the molten salt, which was composed of NaCl and KCl, was dried in vacuum to remove the H and O elements before the electrolysis. After drying, the electrolyzer was heated and then a certain amount of  $\text{TiCl}_4$  was added and reacted with the Ti sponge, forming the  $\text{TiCl}_3$ ,  $\text{TiCl}_2$  and attendant NaCl–KCl– $\text{TiCl}_x$  molten salt. The electrolysis experiment was performed by direct-current power supply at Ar protecting atmosphere. The electrolysis temperature was 500–800 °C. The electrolysis time was 28–41 h. When the electrolysis was finished, the anode and the cathode were all shifted up immediately from the molten salt. At last, the electrolysis product was cleaned to remove the molten salt and obtain Ti powder. After electrolysis, the

elemental compositions were detected by inductively coupled plasma-atomic emission spectrometry (ICP-AES), glow discharge mass spectrometry (GD-MS) and electron probe micro-analysis (EPMA). The morphology of titanium powder was analyzed by scanning electron microscopy (SEM). The valence state was analyzed by X-ray photoelectron spectroscopy (XPS). The inner microstructure of electrodeposited titanium was characterized by focused ion beam (FIB) and transmission electron microscopy (TEM), and high-resolution transmission electron microscopy (HRTEM) with selected area electron diffraction (SAED) pattern.

## 3 Results and discussion

### 3.1 Ti valence states evolution

In order to disclose the valence state evolution of Ti ion, the molten salts were extracted for XPS analysis at electrolysis time of 10, 20 and 30 h respectively, and the results are shown in Fig. 2. The various valences and contents of titanium at different electrolysis stages are listed in Table 1. At electrolysis time of 10 h, there are two peaks, indicating the existence of +3 and +4 valences of titanium (Fig. 2(a)). When the electrolysis time is extended to 20 h, there are four peaks and at least three kinds of valence, corresponding to +1, +3 and +4 valences (Fig. 2(b)). When the electrolysis time is further increased to 30 h, the three Ti peaks reveal the valence states of +1 and +3.

At the earlier stage of electrolysis, the main valence of Ti is +4 with the content of 87.6%, and the Ti content of +3 valence is only 12.37%, while there is no existence of +2 valence Ti. It can be understood by considering the chemical reaction equilibrium constants between Ti ion and Ti, as shown in Table 2. There are four chemical reactions between Ti ion and Ti. It can be seen that the equilibrium constant of +2 valence Ti generation is lower

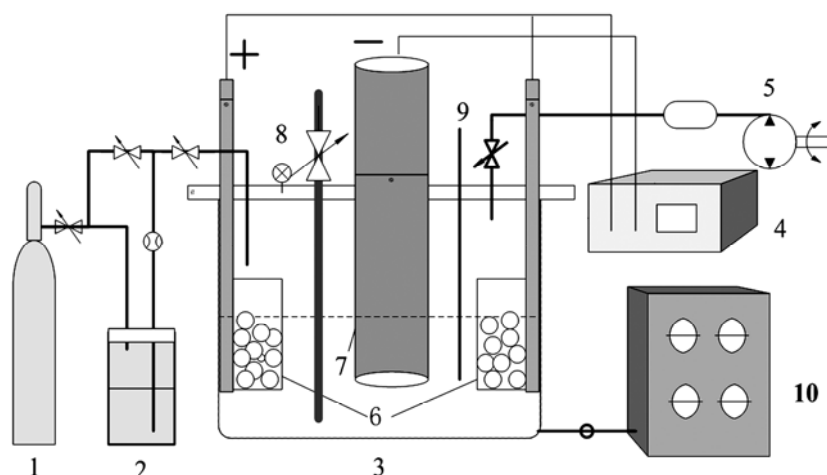


**Fig. 1** Apparatus diagram of molten salt electrolysis: 1—Ar gas; 2— $\text{TiCl}_4$  storage tank; 3—MSE refining slot; 4—DC power supply; 5—Vacuum pump; 6—Anode basket; 7—Cathode plate; 8—Vacuum gauge; 9—Thermocouple; 10—Temperature control device

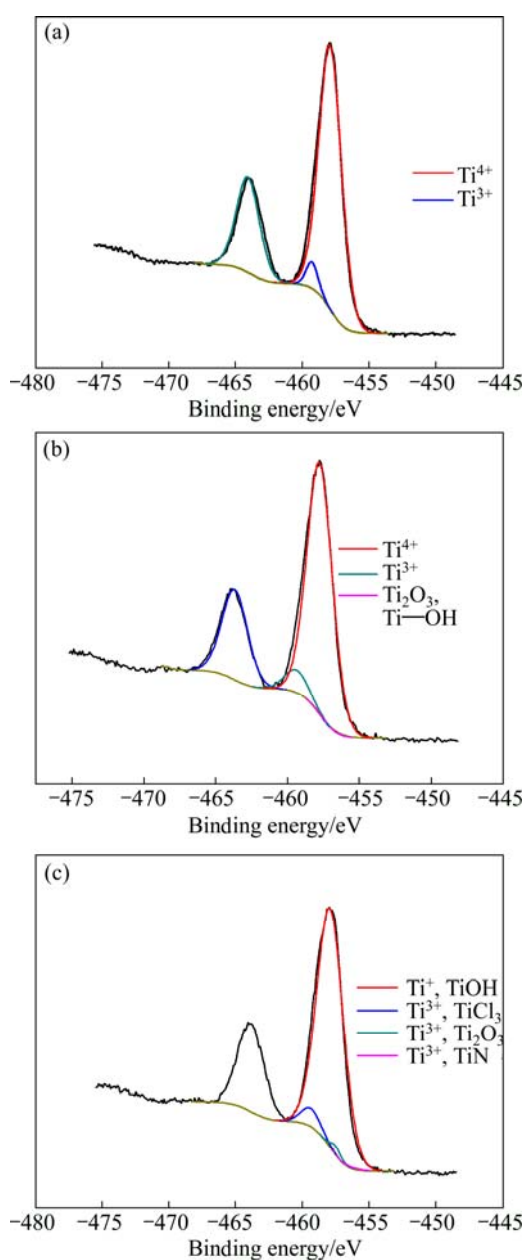


**Fig. 2** XPS patterns of Ti element in molten salt at different electrolysis times: (a) 10 h; (b) 20 h; (c) 30 h

**Table 1** Titanium valence of molten salt at different electrolysis times

Electrolysis time/h	Mole fraction/%	Valence	Compound
10	87.6	+4	TiO <sub>2</sub> ,TiCl <sub>4</sub>
	12.37	+3	TiCl <sub>3</sub>
20	80.54	+4	TiO <sub>2</sub> ,TiCl <sub>4</sub>
	18.47	+3	TiCl <sub>3</sub>
	0.43	+1	TiOH
	0.56	+3	Ti <sub>2</sub> O <sub>3</sub>
30	93.05	+1	TiOH
	5.21	+3	TiCl <sub>3</sub>
	1.37	+3	TiN
	0.37	+3	Ti <sub>2</sub> O <sub>3</sub>

**Table 2** Relationship between chemical reaction and equilibrium constant at different temperatures

Reaction	lg K=A+BT <sup>-1</sup>	lg K			
		800 K	900 K	1000 K	1100 K
3TiCl <sub>4</sub> +Ti=	lg K=4.09+				
4TiCl <sub>3</sub>	10347/T				
TiCl <sub>4</sub> +Ti=	lg K=-1.798+				
2TiCl <sub>2</sub>	7968/T	8.16	7.06	6.17	5.45
TiCl <sub>4</sub> +TiCl <sub>2</sub> =	lg K=3.041+				
2TiCl <sub>3</sub>	1194/T	4.53	4.37	4.24	4.13
2TiCl <sub>3</sub> +Ti=	lg K=-5.038+				
3TiCl <sub>2</sub>	6774/T	3.43	2.49	1.74	1.12

than that of +3 valence Ti, inducing the lower production rate of +2 valence Ti. Moreover, the +2 valence Ti can react with oxygen easily and form TiO<sub>2</sub>. As a result, at the earlier electrolysis stage, the main Ti valence is +3 and +4 states. At the medium stage of electrolysis, the content of +3 valence Ti increases to 18.47% and the content of +4 valence Ti faintly decreases to 80.54%, thus the content of +4 valence Ti is still high. It is because the extracted molten salt at high temperature may react with oxygen in air, which results in the oxidization of +2 valence Ti and hydrolysis, forming the TiOH. At the later electrolysis stage, the main Ti valence is +1 and the content of TiOH is as high as 93.05%, which is due to the serious hydrolysis in a moist atmosphere at sampling process from molten salt: 2TiCl<sub>2</sub>+2H<sub>2</sub>O=2TiOH+2HCl+Cl<sub>2</sub>.

### 3.2 Impurity evolution

#### 3.2.1 Impurity in molten salt

Table 3 shows the impurity contents in molten salt extracted at different electrolysis times. It can be seen that there exist different kinds of impurities according to the variation of impurity content. The first kind of impurity is Si element, whose content changes little. It is because Si element mainly exists in oxide and resides in anode mud. The second kinds of impurities are Cr, Mn, Al, which tend to be dissolved accompanying with Ti at the anode, because their anode potentials are close to that of Ti. As a result, the contents of Cr, Mn, Al are almost constant. Pre-electrolysis can remove the above impurities. The third kinds of impurities are Fe, Cu, Ni, whose contents are decreased markedly. The fourth kinds of impurities are O, N, H, whose contents are increased obviously. It is because these elements easily turn into solid solution and oxide with Ti, and reside in molten salt.

#### 3.2.2 Impurities in electrolytic Ti

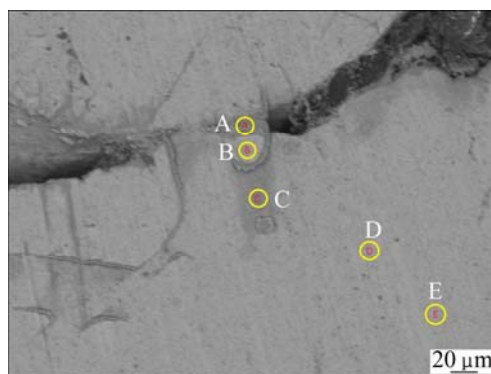
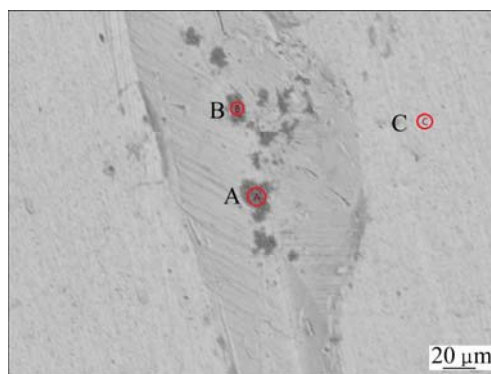
In order to study the existence state, distribution and formation mechanism of impurities, the micro-area chemical composition of electrolytic Ti was analyzed using EPMA. Figure 3 shows the seam of two dendrites,

**Table 3** Element contents in molten salt at different electrolysis time

Impurity	Content/%		
	0 h	20 h	30 h
Al	0.0120	0.0100	0.0110
Cr	0.0035	0.0038	0.0039
Cu	0.0600	0.0170	0.0062
Fe	0.0810	0.0015	0.0012
Mn	0.0001	0.0001	0.0001
Ni	0.0055	0.0010	0.0010
Si	0.0020	0.0019	0.0018
H	0.0130	0.0170	0.0290
O	0.0140	0.5900	0.8900
N	0.0240	0.0580	0.0740

and Table 4 shows the chemical compositions of different zones from Fig. 3. It can be basically concluded that the chemical compositions in seam and interior of dendrites are different. In zones A and C, the chemical compositions are similar and the Ti content is lesser but the O, Fe, Cl contents are higher. It is because zones A and C are seams of two dendrites, in which hydrolysis and oxidation occur easily, forming solid-state  $\text{TiOCl}_2$  and  $\text{TiO}_2$ . It should be noted that the existence of small amount of C element is due to carbon injection treatment of polished sample. In zones B, D and E, the Ti content is relatively high, and the impurity contents are less than those in seam zone.

Figure 4 shows the interior structure of electrolytic Ti crystal. A small amount of tunnel zone can be seen in the crystal. The formation of tunnel zone is due to the collision, contact, and growth, and eventually a closed space forms. The element compositions of the electrolytic Ti interior are shown in Table 5. The zone C

**Fig. 3** BSE image showing seam of two electrolytic dendrites**Fig. 4** BSE image showing interior of electrolytic Ti crystal

is mainly Ti element. The zones A and B contain a large amount of impurities. The main impurities are metal element, oxide and KCl and NaCl. During the crystal growth process, the impurities are surrounded by Ti crystal and reside in crystal interior. Therefore, it can be concluded that the crystal boundary has small tunnel with residual impurities, and with the proceeding of electrolysis, the tunnel number will increase, which is unfavorable for the Ti purity. Overall, the impurities are very easily formed in dendrites seam and crystal tunnel.

**Table 4** Element analysis of seam of dendrites from Fig. 3

Zone	Mass fraction/%								
	O	C	Fe	Ni	Ti	V	Cu	Cr	Cl
A	33.341	0.181	18.652	–	14.757	0.807	0.719	–	6.996
B	8.645	0.209	2.570	–	73.854	3.332	–	0.018	–
C	33.236	0.356	6.604	0.183	39.418	1.705	0.113	–	9.299
D	7.743	0.384	10.724	–	68.458	12.745	0.042	0.102	–
E	6.904	0.348	–	–	88.941	–	–	–	–

**Table 5** Element analysis of interior of electrolytic Ti crystal from Fig. 4

Zone	Mass fraction/%									
	O	C	Fe	Ti	V	Cu	Cr	Cl	K	Na
A	8.464	1.730	2.180	7.706	1.476	0.323	0.071	0.102	–	–
B	5.754	2.067	0.535	6.818	1.374	0.507	–	0.012	0.060	0.058
C	7.665	0.337	0.402	104.544	3.067	0.104	0.043	–	–	–

### 3.3 Electrocrystallization

#### 3.3.1 Effect of temperature

Figure 5 shows the powder characteristics prepared under different electrolysis temperatures. It can be seen that the powder prepared at 750 °C exhibits granular shape, while at higher temperature of 800–950 °C it exhibits dendritic shape. Moreover, the powder size prepared at 750 °C is smaller than that prepared at high temperature of 800–950 °C. The powder size and morphology obtained at temperature of 800–950 °C vary little. This can be understood by considering the relationship between temperature, ion migration rate and concentration polarization. At relatively low temperature of 750 °C, the molten salt

viscosity is higher, which is unfavorable for titanium ion migration, thus causing the concentration polarization and inhibition of crystal growth, and accordingly fine titanium particles. With the elevation of temperature to 800–850 °C, the ion migration rate is accelerated, so the concentration polarization is weakened, resulting in relatively coarser particles. With the further elevation of temperature to 900–950 °C, although the molten salt viscosity is decreased and the ion migration is fast, which is in favor of the growth of deposited powder, the dissolution velocity of deposited titanium by  $\text{TiCl}_4$  is speeded up at such high temperature, thus hindering further coarsening of deposited titanium powder.

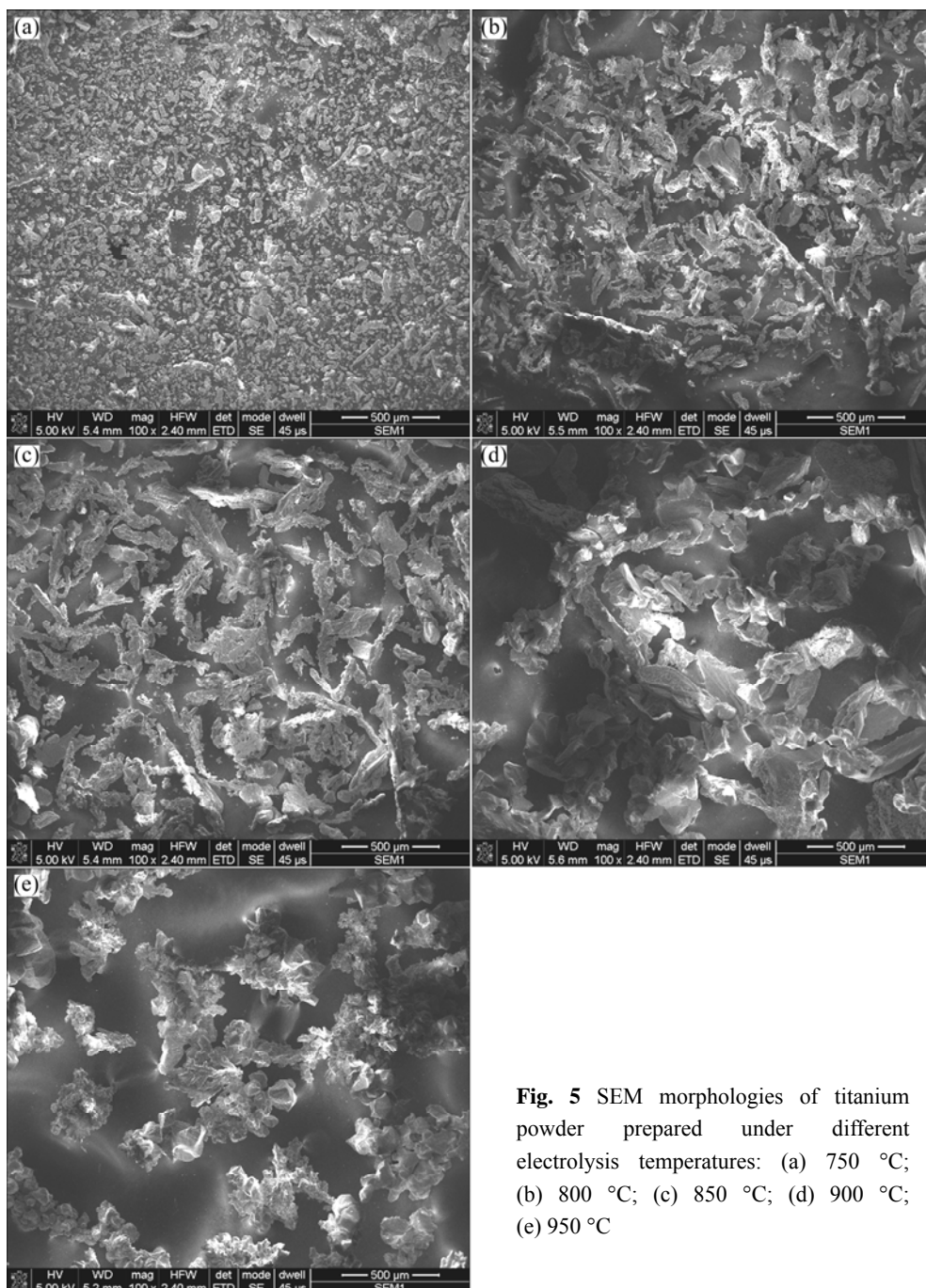


**Fig. 5** SEM morphologies of titanium powder prepared under different electrolysis temperatures: (a) 750 °C; (b) 800 °C; (c) 850 °C; (d) 900 °C; (e) 950 °C

### 3.3.2 Effect of electrolysis time

Figure 6 shows the morphologies of electrodeposited titanium particles at different electrolysis time. After electrolysis for 4 h, many fine titanium filaments are formed and cover on the coarse titanium particles, which are electrodeposited in pre-electrolysis process and contain many impurities (Fig. 6(a)). When the electrolysis time reaches 8 h, the number of titanium filament increases (Figs. 6(b) and (c)). At electrolysis time of 12 h, the particle exhibits dendritic shape and the particle size increases (Fig. 6(d)). With further prolonging time to 16 h, the

electrodeposited titanium has much bigger particle size, with many small protuberance growth on the titanium powder surface (Fig. 6(e)). When the electrolysis time is prolonged to 20 h, the electrodeposited titanium grows continually and collides each other, gathering a block with a smooth surface. The above experimental results can be understood as follows. In this experiment, the pre-electrolysis was firstly conducted for 8 h, in order to remove the crystal water and impurities. This is because the metal impurities, whose deposition potential is appropriate to titanium, are apt to deposit at cathode preferentially, thus the pre-electrolysis is an effective

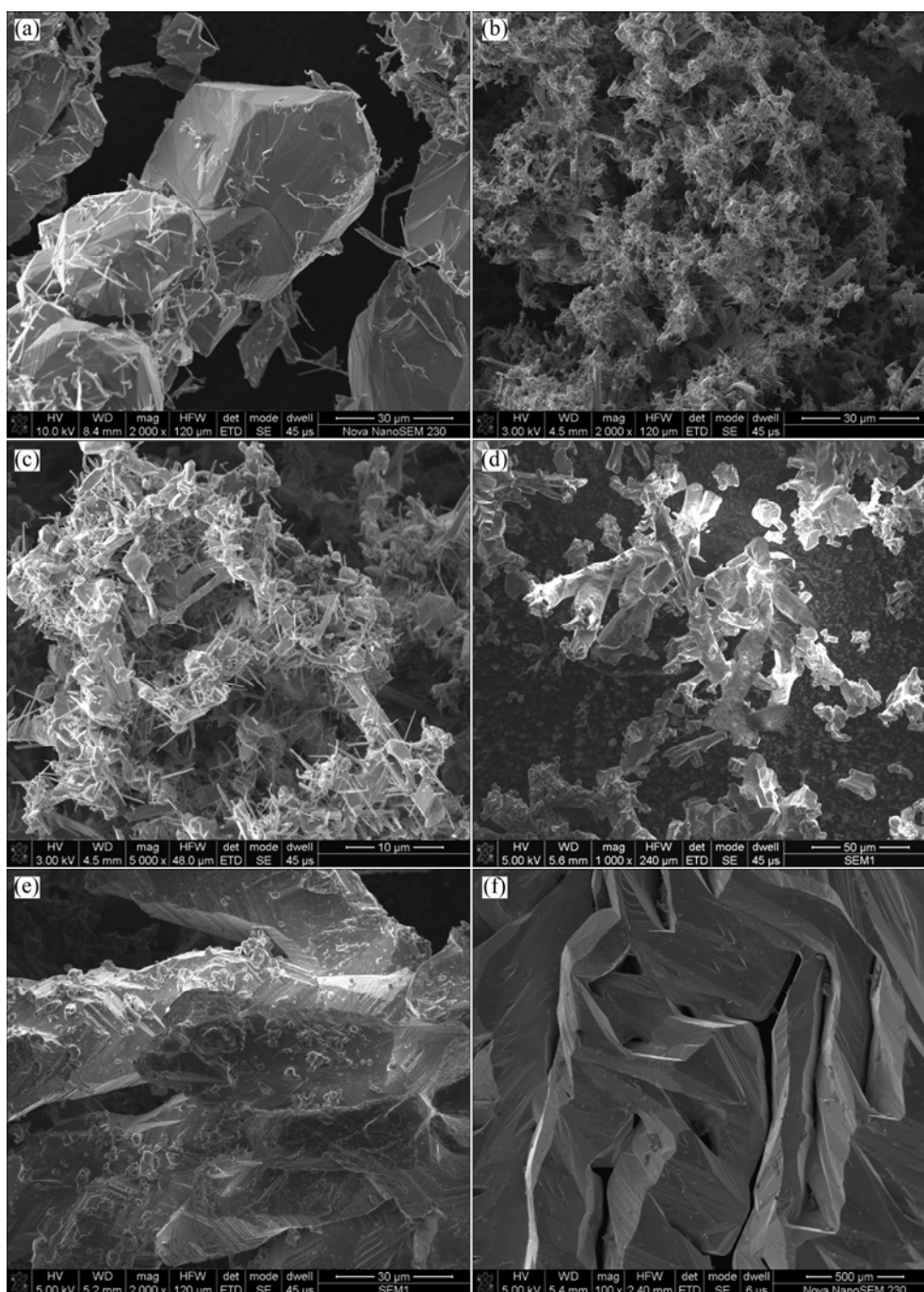


**Fig. 6** SEM morphologies of deposited titanium at different electrolysis time: (a) 4 h; (b, c) 8 h; (d) 12 h; (e) 16 h; (f) 20 h

way to improve the purity of electrolytic titanium. In the pre-electrolysis, there also exist crystal nucleation and growth. The deposited titanium and impurity in the pre-electrolysis can provide the active growth zone, especially the included angle and closed angle zone, in which the surface energy is lower and the nucleation of titanium ion has lower energy barrier. The needle-like or cotton-like titanium crystal is due to the different growth rate at the different zone. Moreover, the titanium growth is spiral growth mode, yielding many footsteps on the surface.

### 3.3.3 TEM analysis

In order to characterize the inner microstructure of electrodeposited titanium, the FIB “lift-out” technique was utilized to prepare TEM sample. For the purpose of preventing contamination, the TEM specimen was mounted onto the Cu grid. Figure 7(a) shows the TEM image of electrodeposited titanium. It can be seen that the electrolytic titanium powder is not a single crystal, but contains many nanostructured grains and subgrains, with grain size of 100–500 nm. Figure 7(b) shows the SAED pattern, showing the  $[3\bar{5}1]$  crystal zone axis of close-packed hexagonal titanium. Figure 8 shows the HRTEM images of electrolytic titanium. It shows that the interatomic layer distance is 0.256 nm and the crystal face is  $(01\bar{1}0)$ , which confirm the close-packed hexagonal titanium.

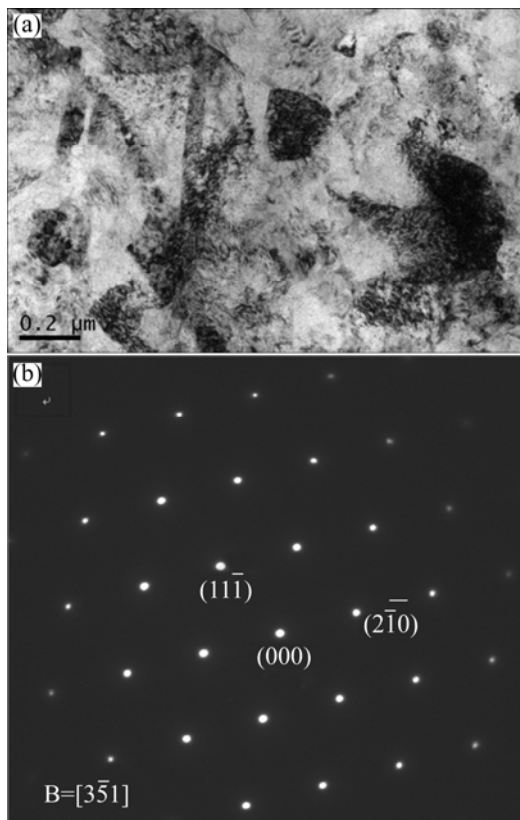


**Fig. 7** TEM image (a) showing crystal structure of molten salt electrodeposited titanium and SAED pattern (b)

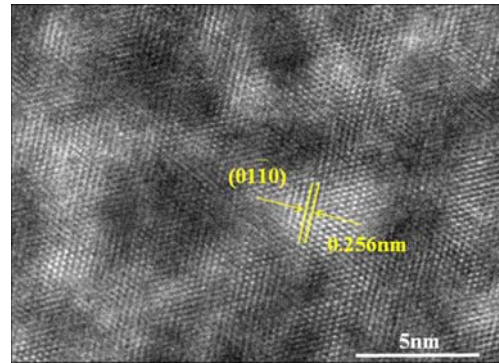


**Fig. 8** HRTEM image showing crystal structure of molten salt electrodeposited titanium

## 4 Conclusions

1) At the earlier electrolysis stage, the titanium valence is mainly +4. At the medium stage, the titanium valence is mainly +3. At later stage the titanium valence is mainly +2.

2) During the electrolysis process, the impurity Si content varies little, the contents of impurities Cr, Mn, Al are almost constants, the contents of impurities Fe, Cu, Ni decrease markedly, and the contents of impurities O, N, H increase obviously.

3) The residual impurities are usually distributed in small tunnel of dendritic crystals, and with the proceeding of electrolysis, tunnel number will increase, which is unfavorable for the purity.

4) The electrolysis temperature and time all have obvious influence on electrolytic titanium morphologies. The powder size prepared at 750 °C is lower than that prepared at high temperature of 800–950 °C. The powder size and morphology obtained at temperature 800–950 °C vary little. Prolonging the electrolysis time can increase the titanium particle size.

5) TEM observation shows that the electrodeposited titanium is not a single crystal, but contains many nanostructured grains and subgrains, with grain size of 100–500 nm.

## References

- [1] ZHANG W S, ZHU Z W, CHEN C Y. A literature review of titanium metallurgical processes [J]. Hydrometallurgy, 2011, 108(3–4): 177–188.
- [2] YUAN T C, WENG Q G, ZHOU Z H. Preparation of high-purity titanium by molten-salt electrolysis process [J]. Advanced Materials Research, 2011, 284–286: 1477–1482.
- [3] CHEN X H, WANG H, LIU Y M. Thermodynamic analysis of production of high purity titanium by thermal decomposition of titanium iodide [J]. Transactions of Nonferrous Metals Society of China, 2009, 19(5): 1348–1352.

- [4] NAGESH C, RAO C S, BALLAL N B. Mechanism of titanium sponge formation in the Kroll reduction reactor [J]. Metallurgical and Materials Transactions B, 2004, 35(1): 65–74.
- [5] LEE J C, SOHN H S, JUNG J Y. Effect of  $TiCl_4$  feeding rate on the formation of titanium sponge in the Kroll process [J]. Korean Journal of Metals and Materials, 2012, 50(10): 745–751.
- [6] VAN D S, OOSTHUIZEN S J, HEYDENRYCH M D. Titanium production via metallothermic reduction of  $TiCl_4$  in molten salt: Problems and products [J]. Journal of The South African Institute of Mining and Metallurgy, 2011, 11(3): 141–148.
- [7] CUEVAS F, FERNANDEZ J F, SANCHEZ C. Kinetics of the iodide titanium process by the thermal decomposition of titanium tetraiodide [J]. Journal of the Electrochemical Society, 2000, 147(7): 2589–2596.
- [8] OH J M, LEE B K, PARK H K. Preparation and purity evaluation of 5N-grade ruthenium by electron beam melting [J]. Materials Transactions, 2012, 53(9): 1680–1684.
- [9] WANG Q Y, SONG J X, HU G J. The equilibrium between titanium ions and titanium metal in NaCl–KCl equimolar molten salt [J]. Metallurgical and Materials Transactions B, 2013, 44(4): 906–913.
- [10] WENG Q G, LI R D, YUAN T C, ZHOU Z H, HE Y H. Investigation to impurity content and micromorphology of high purity titanium powder prepared by molten salt electrolysis [J]. Materials Research Innovation, 2013, 17(6): 396–402.
- [11] CHEN G Z, FRAY D J, FARTHING T W. Direct electrochemical reduction of titanium dioxide to titanium in molten calcium chloride [J]. Nature, 2000, 407(6802): 361–364.
- [12] FRAY D J. Novel methods for the production of titanium [J]. International Materials Reviews, 2008, 53(6): 317–325.
- [13] SUZUKI R O. Calciothermic reduction of  $TiO_2$  and in situ electrolysis of CaO in the molten  $CaCl_2$  [J]. Journal of Physics and Chemistry of Solids, 2005, 66(2–4): 461–465.
- [14] JACOB K T, GUPTA S. Calciothermic reduction of  $TiO_2$ : A diagrammatic assessment of the thermodynamic limit of deoxidation [J]. JOM, 2009, 61(5): 56–59.
- [15] PARK I, ABIKO T, OKABE T H. Production of titanium powder directly from  $TiO_2$  in  $CaCl_2$  through an electronically mediated reaction (EMR) [J]. Journal of Physics and Chemistry of Solids, 2005, 66(2–4): 410–413.

## 海绵钛熔盐电解制取高纯钛粉过程中 离子价态、杂质及电结晶行为

翁启刚, 李瑞迪, 袁铁锤, 李健, 贺跃辉

中南大学 粉末冶金国家重点实验室, 长沙 410083

**摘要:** 以 NaCl–KCl– $TiCl_x$  为电解质, 以海绵钛为原料进行熔盐电解提纯制取高纯钛粉。研究电解过程中离子价态、纯度及电结晶的演变规律。XPS 分析表明, 在电解前期、中期及后期, 钛离子主要分别以+4、+3、+2 价存在。在电解过程中, Si、Cr、Mn、Al 杂质的含量基本恒定, 而 Fe、Cu、Ni 杂质的含量逐渐降低, O、N、H 元素的含量明显增加。在电解钛粉体内部, 杂质元素主要分布在枝晶间所形成的“坑道”内。电解钛粉体形貌及粉体粒度受电解温度和时间的影响较大, 温度升高及时间延长可增加钛粉体的粒度。透射电镜分析表明, 电结晶的钛粉体不是单晶, 而是由大量的纳米晶粒及亚晶粒组成的, 晶粒尺度为 100–500 nm。对电解机理进行了讨论。

**关键词:** 熔盐电解; 高纯钛; 粉末; 价态; 电结晶

(Edited by Sai-qian YUAN)